Combinatorics and Frequency Distributions as the Determining Factors of Electron and Nuclear Spectra

Anatoly V. Belyakov

Tver, Russia. E-mail: belyakov.lih@gmail.com

It has been established that electronic and nuclear spectra can be calculated and formed using combinatorics and frequency distributions (FD) provided that electrons, nucleons and other elementary particles in the composition of an atom are represented as unit structureless elements. The examples given show a good match between the calculated spectra and the experimental ones. The program for calculating spectrograms has been compiled.

1 Introduction

Electronic and nuclear spectra are characterized by a set of emission (absorption) spectral frequency lines arising from the excitation of atoms or by the energy spectrum of split off nucleons in the nuclear decay process. In electronic spectra the spectral lines position for hydrogen and for hydrogen-like atoms is determined by the Balmer-Rydberg formula for the radiation wavelength

$$\lambda_e = \frac{n^2 m^2}{m^2 - n^2} \frac{1}{R_\infty Z^2}, \qquad (1)$$

where n and m are the quantum numbers or orbit numbers, R_∞ is the Rydberg constant, Z is the element atomic number.

For other spectral transitions in multielectron atoms the Rydberg formula gives incorrect results, since the internal electrons screening varies, and for external electrons transitions it is not possible to make a similar correction in the formula to compensate for the nuclear charge weakening, as described above. Therefore, in the general case, to find the position of spectral lines, the Ritz combination principle [1], which has become the basis of modern spectroscopy, is used. Its validity has been confirmed by numerous experimental data. But it is not clear what regularities underlie it, what processes exactly exist, and how the atom internal structure is rearranged in order to cause the waves emission with a frequency corresponding to any spectral line.

Nuclear spectra arise when a nucleus is exposed to hard radiation or high-energy electrons. The nucleons split off in this case have the energy of tens of MeV and form the giant dipole resonance (GDR) [2]. The giant resonance is inherent in all nuclei, it has been studied since 1947 and it manifests itself so brightly and universally that, perhaps, not a single nuclear "event" can compare with it. The giant resonance nature is believed to lie in the nucleus dipole oscillations (displacement of all nucleus protons relative to all its neutrons) under the action of long-wavelength γ-radiation. When irradiated with electrons having an energy of more than 200 MeV, along with dipole vibrations, other types of vibrations can also be excited in the nucleus. These vibrations are of a collective nature and form giant multipole resonances (GMRs) [3]. The photonucleons energy spectra are not described by smooth curves, and when studying the cross sections for the (γ, n) reactions, maxima of the first and subsequent orders are found, forming the GDR structure of three types: rough (gross), intermediate, and fine.

There are several GDR theories, the most detailed being the multiparticle shell model [4]. Its development proceeds through a unified description of various collective motions (rotations, surface oscillations, nucleus dipole oscillations), as well as interactions between them. At present, theories are not yet able to give a good quantitative description of the width and fine structure of the giant resonance and the entire spectrum of nucleons separated during the nuclei decay, since there are large computational difficulties and a lack of reliable information about a number of important parameters of the theory.

2 Initial conditions

In this article, as in previous works, in accordance with the mechanistic interpretation of J. Wheeler's idea, charged particles are considered to be the singular points on the three-dimensional surface of our world (conditionally this is the X-region), connected by vortex tubes (current lines of force) through an additional dimension (conditionally this is the Y-region), which is responsible for the electromagnetic forces and the "hidden" mass of the microparticles [5, 6].

If, as is commonly believed, the microparticles are oscillators, then the atom itself can be considered as a collective oscillator, which consists of the "oscillator-electrons" (X-region) and the "oscillators-protons" (Y-region), and these oscillators are elastically connected to each other by the vortex current tubes. At that, according to [7], the electrons located at the more distant orbits are associated with the protons located at the deeper nucleus levels; thus the layers or envelopes are formed in the nucleus that similarly to the electronic shells.

The multielectron atoms protons number's increasing in proportion to the atomic number Z increases the bonds inflexibility, as if "stretching" the vortex tubes, which reduces the oscillators-electrons wavelength in the X-region in accor-

dance with the formula (1). At the same time, the protons mass's increasing reduces the system as a whole inflexibility, therefore in the same proportion increases the oscillator-protons wavelength in the Y-region.

For multielectronic atoms, the numbers m and n lose their meaning of the electron shell number, and n must be taken equal to Z, since in the limit, when $m \to \infty$ and $n = Z$, in accordance with (1), $\lambda \to 1/R_\infty$, and the atom becomes hydrogen-like one. For the radii smaller than $1/R_\infty$, i.e. when there is "sinking" into the Y-region, quantum numbers formally become inverses of n and m, and the formula (1) for oscillator-protons takes the form

$$\lambda_p = \frac{1}{m^2 - n^2} \frac{Z^2}{R_\infty} . \qquad (2)$$

The dependence of wavelengths on Z^2 is understandable, since, unlike a simple one-dimensional oscillator, where the oscillation period depends on its inflexibility and on its mass to the power of 1/2, the atom (taking into account the additional degree of freedom in Y) is a four-dimensional oscillator and $(Z^{1/2})^4 = Z^2$.

3 Formation of the electronic spectra

The spectra revealed in physical experiments is obvious to be as a joint result of the electronic and proton oscillators oscillations superposition; it is clear that in this case, as a result of interference, both damping and amplification of certain frequencies of the spectrum occur. Therefore, to obtain the spectrum, it is necessary to calculate all possible wavelengths of oscillators-electrons according to (1), as well as all possible wavelengths of oscillators-protons according to (2) for all combinations of n and m, and multiply the results logically.

For this purpose, a calculation program has been drawn up (see Appendix). The essence of the program is as follows: to divide a certain spectrum region into intervals, to calculate the *frequency distributions* (FD) of all functions values according to (1) and (2) in the spectrum selected region, write them into the corresponding arrays and multiply these arrays. The type of the spectra obtained by this program depends on the number of values λ_i falling into the i-th interval (i.e., on the parameter q value in the program) and can have the histogram form of different detail (q-large) or the line spectra form (q-small) [8]. Moreover, the type of histograms can reflect some additional spectrum parameters, since the histogram peaks height is proportional to the probability (intensity) of the corresponding spectral parameter along the Y-ordinate.

Fig. 1 shows the experimental spectrum of the holmium liquid filter (240–650 nm) which is a solution of holmium dissolved in perchloric acid for checking the wavelength accuracy [9], and Fig. 2 shows the calculated histogram for $_{67}$Ho. Here and below, the intervals for substituting variables a and b in the calculation program are indicated.

Fig. 3 shows part of the $_{80}$Hg spectrum as a line spectrum. Above it, the spectral lines experimental values are shown

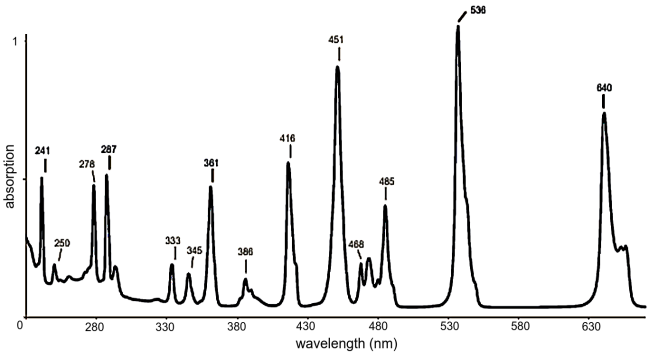

Fig. 1: Typical spectrum of holmium liquid filter (240–650 nm) [9] consists of a solution of holmium dissolved in perchloric acid.

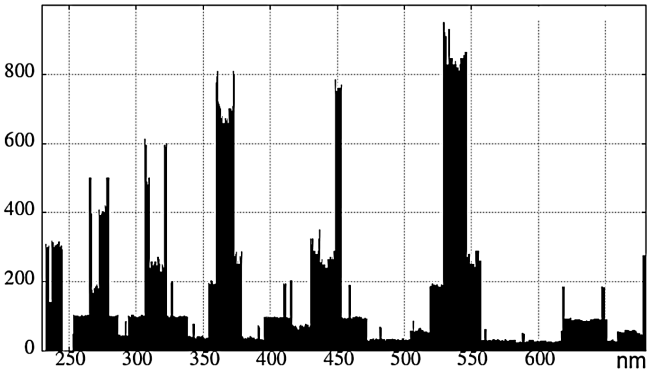

Fig. 2: Calculated spectrum for $_{67}$Ho: $q = 0.026$, $\lambda_t(a,b) = 57$–67, $\lambda_p(a,b) = 1$–67.

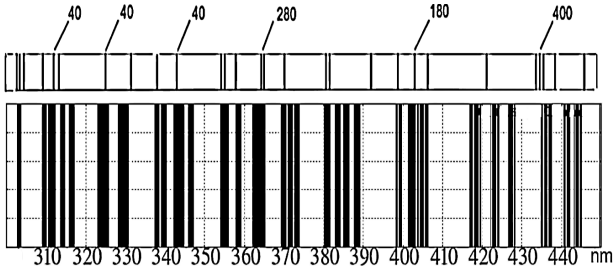

Fig. 3: Calculated spectrum for $_{80}$Hg: $q = 0.0021$, $\lambda_e(a,b) = 50$–80, $\lambda_p(a,b) = 1$–80.

and the brightness values of some of them are given. Note, when changing the interval of substitution of variables the histograms shape changes; in the case of a line spectrum it affects the spectral lines intensity, the presence or absence of some lines, but their position in the spectrum does not change.

Obviously, the constructed spectra are in good agreement with the experimental ones. Of course, one cannot expect the calculated spectra to match exactly with the experimental ones, since the latter are influenced by various factors: the methods of excitation of atoms, the degree of their ionization, the presence of forbidden transitions, the medium which the element is locate in, etc.

Nevertheless, in a number of cases, for some sets of variables, even the external shape of the calculated non-line spectra (the histograms shape) is very similar to the real non-line spectra (see Figs. 1 and 2), which, apparently, corresponds to certain physical conditions. Thus, limiting the function λ_e to variables within 57–67 means that when calculating the spectrum only the electrons in the outer shells of $_{67}$Ho (10 units) are taken into account. Indeed, it is known the inner shells electrons do not take part in the formation of the visible spectrum range for atoms having high numbers Z. For the $_{80}$Hg spectrum 30 electrons are taken into account. This turned out to be sufficient to form the spectrum. With a full set of variables, the short-wavelength spectrum part is enhanced and, in general, the spectrum detail is enhanced.

4 Formation of the nuclear spectra

The region of the giant dipole resonance extends within the energy range of tens of MeV, and its shape and structure are extremely diverse. When the nucleus is exposed to gamma radiation or high-energy electrons, there is both protons and neutrons's splitting off. Thus, the nucleus as an oscillator should contain the maximum number of unit elements (oscillators-nucleons) equal to its mass number A. On the other hand, by analogy with oscillators-electrons, one can imagine that there are oscillators-pions or other mesons, which, as expected, exist in the proton close environment in the form of a virtual meson "coat" [10].

So, to build a nuclear spectrum one should use the same formulas (1) and (2), replacing the element number Z with the mass number A, but at the same time, as it were, "going deeper" along the Y-axis, that is, moving to smaller sizes and higher energies. The transition coefficient, as it turned out, is equal to a^3 — the fine structure constant in the cube $(1/137)^3$. Thus, for the nuclear resonance wavelengths, denoting them λ_π and λ_n, we have

$$\lambda_\pi = \frac{a^3 n^2 m^2}{m^2 - n^2} \frac{1}{A^2 R_\infty}, \tag{3}$$

$$\lambda_n = a^3 \frac{1}{m^2 - n^2} \frac{A^2}{R_\infty}. \tag{4}$$

These formulas, passing to the frequencies and further to the energies in MeV, are written as

$$E_\pi = \frac{m^2 - n^2}{n^2 m^2} \frac{A^2 R_\infty c h}{a^3 k}, \tag{5}$$

$$E_n = \left(m^2 - n^2\right) \frac{R_\infty c h}{a^3 k A^2}, \tag{6}$$

where c is the light speed, h is the Planck's constant, k is the conversion factor 1.602×10^{-13} [J/MeV]. Calculating the constants, we get

$$E_\pi = 35.02\, A^2 \frac{m^2 - n^2}{n^2 m^2}, \tag{7}$$

$$E_n = 35.02 \frac{m^2 - n^2}{A^2}. \tag{8}$$

The general view of the giant resonance for light and heavy nuclei, obtained from the calculation in accordance with (7) and (8), is shown in Fig. 4, which generally agrees with the experimental results. Indeed, in the experiments with irradiation of the nuclei with low mass numbers, even at low resolution, maxima are found in the giant resonance, in contrast to the heavy nuclei, where numerous weak peaks are detected only at high resolution.

The giant resonance has been established to be formed in the heavy nuclei with the participation of nucleons from the two outermost nuclear shells, while the main nucleon core lying under the outer shells is not affected at all by the photo disintegration process. At that, with an increase in the mass number A, the neutron fraction knocked out of the nucleus increases, while the proton fraction decreases, reaching only about 1% in a nucleus with $A \approx 200$ [11].

Therefore, if one takes into account only those nucleons (neutrons) that are not included in clusters and therefore easily splitting off from the nucleus (for Pb^{207}, as indicated in [7], there are 65 units), then when forming a spectrogram for Pb^{207}, one should limit the variables range for E_n within 142–207. In this case, the maximum of the spectrogram shifts to the range of 11–12 MeV and it takes the form close to the Poisson distribution; this is generally match to the experimental data. As in the case of the electronic spectrum, this is, as it were, the formal restriction on the range of variables, coincides with the physical meaning of the phenomenon, otherwise the GDR peak would be shifted towards higher energies.

Fig. 5 shows the experimental cross sections for reactions $Al^{27}(p, \gamma_0)Si^{28}$ according to [12], and Fig. 6 shows the calcu-

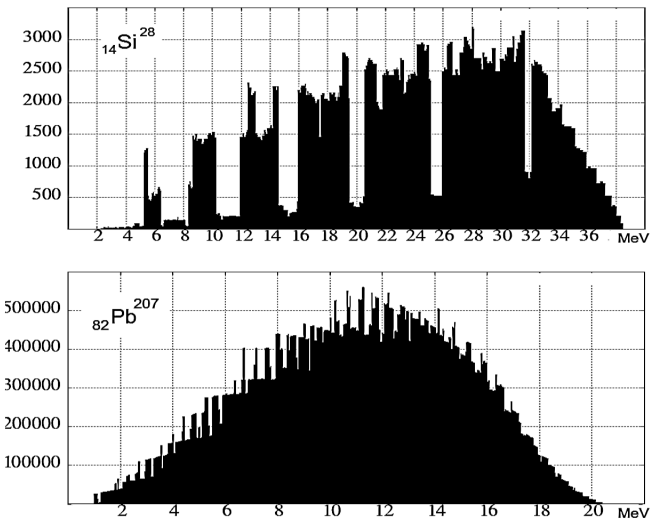

Fig. 4: General view of the GDR for light and heavy nuclei : $q = 0.1$, $A = 28$: $E_\pi, E_n(a, b) = 1$–28, $A = 207$: $E_\pi(a, b) = 1$–207, $E_n(a, b) = 142$–207.

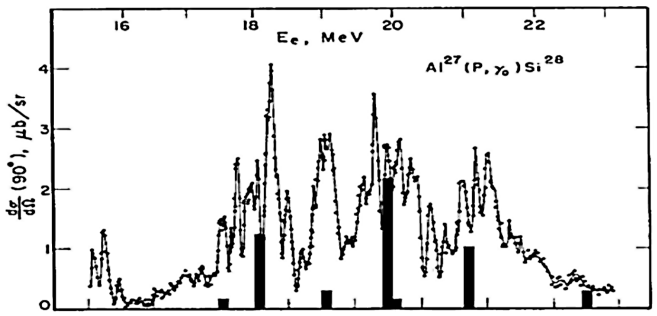

Fig. 5: Reaction cross sections Al^{27} (p, γ_0) Si^{28} [12] and data of theoretical calculations photodisintegration within the multiparticle shell model.

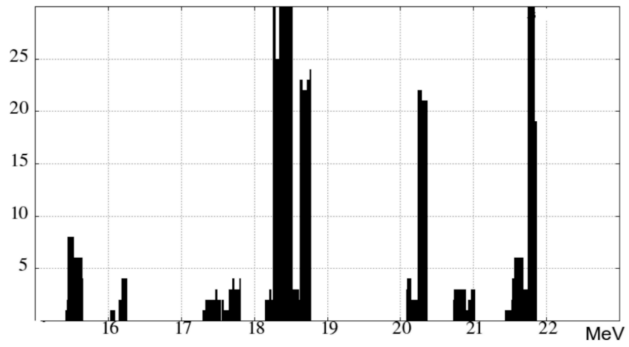

Fig. 6: Calculated spectrum for Al^{27} Si^{28}: $A = 27.5$, $q = 0.007$, $E_\pi, E_n(a, b) = 1$–27.

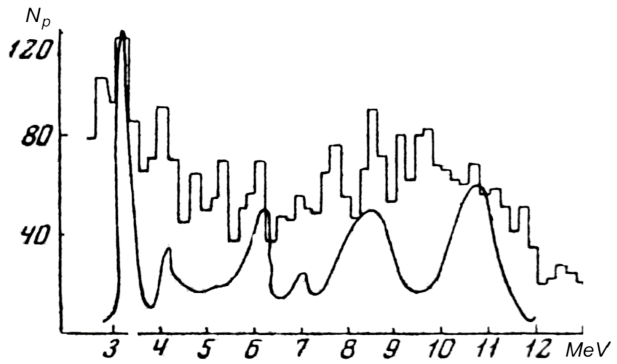

Fig. 7: Spectrum of photoprotons from Ca^{40} upon irradiation with the bremsstrahlung spectrum of γ-quanta with $E_{\gamma max} = 25$ MeV and calculated spectrum in the shell model (smooth curve).

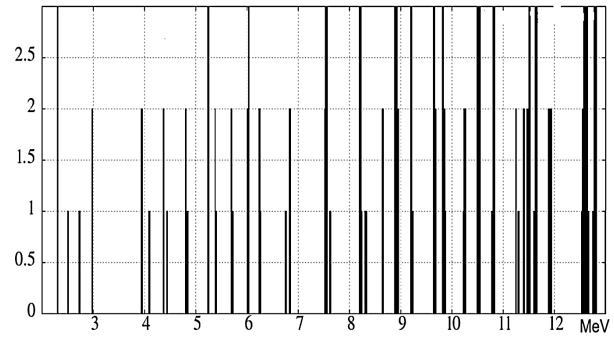

Fig. 8: Calculated spectrum for Ca^{40}: $q = 0.003$, $E_\pi, E_n(a, b) = 1$–40.

lated spectrogram in the histogram form. Obviously, the main peaks of the reaction cross section (p, γ_0) coincide with those in the calculated spectrogram. At the same time, a large number of narrow peaks with a width of 50–100 keV are observed in the reaction cross section against the intermediate structure background (resonances with a width of 0.4–1.0 MeV). The existing theory does not explain the nature of these peaks. But in the calculated spectrograms they are revealed as the parameter q decreases. These coincidences point to the manifestation of combinatorics, to the fact that any maximum is not the result of any particular resonance, but the superposition of many single events.

Fig. 7 shows the experimental spectrum for Ca^{40} [13], and Fig. 8 shows the calculated spectrogram. It also demonstrates good agreement with the experimental data both in terms of the peaks number and the peaks positions for Ca^{40}.

In the process of the studying the atomic nuclei structure by the method of scattering of electrons with energies up to 225 MeV new giant multipole resonances (GMR) were discovered. These resonances go beyond the GDR, which arise during photodisintegration. They have a much more complex structure than that obtained from photonuclear experiments and theoretical predictions. To explain them, quadrupole, octupole, and other types of oscillations was assumed can be excited in the nucleus.

The parameters of the giant resonance in Fe^{56} E_{res}, MeV are given in [3, p. 142] (the plus or minus errors in absolute value are shown in parentheses):

9.5 (0.1)	10.1 (0.1)	10.3 (0.3)	11.3 (0.5)
11.9 (0.9)	13.0 (0.3)	13.0 (0.9)	13.1 (0.1)
14.6 (0.3)	15.0 (0.4)	15.6 (1.2)	16.0 (0.2)
16.1 (0.5)	16.3 (0.1)	16.9 (0.1)	17.3 (0.1)
17.9 (0.2)	18.2 (0.1)	18.3 (0.1)	19.0 (0.5)
19.8 (0.3)	23.9 (0.3)		

On Fig. 9 the calculated spectrogram for Fe^{56} is shown. It can be seen that almost all of the above energy values, within the limits of errors, coincide with the peaks of the first (most) and second orders in the calculated spectrogram.

On Fig. 10 a part of the spectrogram for Fe^{54} in the line spectrum form is shown. Here is a good agreement with experimental data [3, p. 149] too:

Of course, as in the case of electronic spectra, the calculated nuclear spectrograms cannot completely coincide with the real ones, because in addition, there is an incomplete agreement between the data of different experiments. The

9.7 (0.1)	12.4 (0.5)	12.6 (0.4)	13.4 (0.2)	13.8 (0.2)
15.0 (0.9)	15.0 (1.3)	17.5 (0.2)	17.9 (0.2)	19.2 (0.1)
20.2 (0.1)	20.3 (0.1)	23.9 (0.3)	25.4 (0.4)	

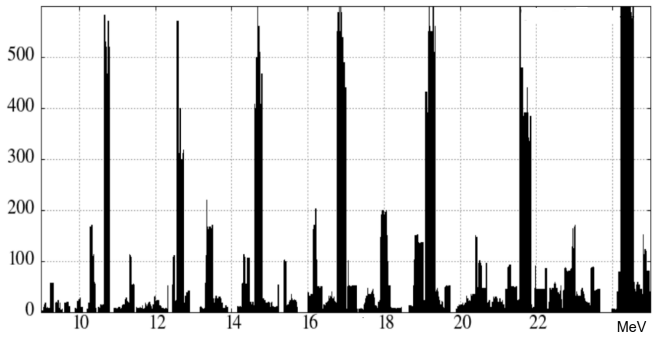

Fig. 9: Calculated spectrum for Fe^{56}: $q = 0.005$, $E_\pi, E_n(a, b) = 1$–56.

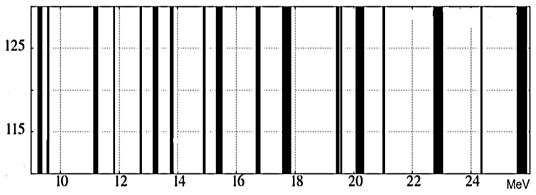

Fig. 10: Calculated spectrum for Fe^{54}: $q = 0.007$, $E_\pi, E_n(a, b) = 1$–54.

instrumental functions of the experiments have very complex shapes, so that the determined cross sections differ in all the main parameters (shape, size, and energy position). It should also be noted that in the above method for calculating spectrograms, the mass number A is the sum of neutrons and protons, and the spectrograms do not differ for nuclei with the same A. The accuracy of the calculated spectra can be improved by introducing additional restrictions or additions to the set of variables.

Nevertheless, the obtained results show this method of analysis can be used as an addition to the instrumental spectrography methods, since it makes it possible to quickly, almost instantly find the statistically most probable form of electronic and nuclear spectra.

5 Conclusions and generalization

The main conclusion from the foregoing is not so much the fact of the emergence of a new analytical method, but that it is possible to obtain results close to reality by considering the complex structure of electronic and nuclear shells as a set of structureless single uniform elements. This contradicts the quantum provisions, according to which elementary particles differ in a set of quantum numbers. On the other hand, each element acquires individuality, since it (and all of them at the same time) moves in the space of variables $n_i - m_i$, and any movement of any element is accompanied by the release of an individual portion of energy E_i, which, being mutually superimposed, eventually form the spectrum. But this again contradicts the quantum principle, this time it contradicts the principle of indistinguishability of identical particles.

Applying a FD to an array of values of the functions E_π and E_n, i.e. to just a set of numbers, gives physically reliable results, but this fact should not be surprising. So in the work of S. E. Shnoll [13], when processing the FD of the experimental data array of the various physical processes, obtained initially in the normal distributions form, these distributions was found are discrete and depend on the algorithms that determine these processes.

The fact that simple formulas for the i-th wavelength or the energy value give results, otherwise obtained through the laborious experiments and complex calculations, leads to the question — do dipole and other resonances affect the nuclear spectra and do they exist in the nucleus at all? Is it really necessary to calculate the nuclear spectra consider nuclei and their components to be the sources of oscillations, or is a set of statistical methods sufficient? This question can only be answered by further wide application of the method described both to the electronic and nuclear spectra and to other physical phenomena in those cases, where it is possible to apply the FD to the functions describing these phenomena.

But now, summing up the above, we can conclude:

— the electronic spectra are reproduced at a deeper level of matter in the nuclear spectra form,

— the type of spectrograms is mainly determined by combinatorics and the frequency distributions of elementary particles, considered as structureless unit elements in the range of their atomic numbers or their mass numbers.

Appendix

A C++ program is written to calculate the wavelength in nanometers. When calculating nuclear spectra, the atomic number Z is replaced by the mass number A, and M is a dimensional coefficient.

```
#include <iomanip>
#include <stdlib.h>
#include <algorithm>
#include <stdio.h>

using namespace std;
struct preobr: binary_function <double, double, double> {
double operator()(double x, double y) const {return x*y;} };

float R, M;
float f1(float x, float y, float z) { return M*(x*x*y*y)
/(y*y – x*x)/z/z/R ;};
float f2(float x, float y, float z) { return M*z*z/(y*y – x*x)/R ;};

FILE *fp = fopen("uuu", "w");

int main() {
```

```
int n=1000000; float*m1 = new float[n]; float*my1 = new float[n];
float*my2 = new float[n]; float*my12 = new float[n];

for (int c=0; c<n; c++) m1[c]=my1[c]=my2[c]=my12[c]= 0;

float z=80, xn=300, xm=500, q=0.002, t=0, c=0; int j=0;
R=1.0974e+7, M=1e+9;
// xn and xm — range limits

for(t=xn; t<xm; t=t+0.001*t) {
j++, m1[j] = t;
// dividing the range into segments
// proportional to its current value

for(int a=1; a<=80; a++) {
for(int b=1; b<=80; b++) {

if(b>a) c = f1(a,b,z);

if(fabs(m1[j] – c) < fabs(q*c)) my1[j]++ ;
// recording the number of values in intervals for f1
}
}
for(int a=1; a<=80; a++) {
for(int b=1; b<=80; b++) {

if(b>a) c = f2(a,b,z);

if(fabs(m1[j] – c) < fabs(q*c)) my2[j]++ ;
// recording the number of values in intervals for f2
}
}
}
transform(my1, my1+j, my2, my12, preobr());

for(int i=0; i<j; i++) {
if(m1[i]!=0)

fprintf(fp, "%20f %20f\n", m1[i], my12[i]);
// writing results to the file "uuu"

std::cout << m1[i] <<" "<< my12[i] << std::endl;
// outputting results to the terminal

}
}
```

Submitted on February 18, 2022

References

1. Ritz W. On a new law of series spectra. *Astroph. Journal*, 1908, October, v. XXVIII, issue 3, 237–243.
2. Bergere R. Features of the Giant E1 Resonance. In: Lecture Notes in Physics, v. 61. Photonuclear Reactions I, Springer-Verlag, Berlin-Heidelberg-New York, 1977.
3. Aizatski N. I., Afanasiev S. N., Buki A.Yu., et al. A Study of Atomic Nuclei Using the Electrons and Photons at Energies Upto 300 MeV. Kharkov, Kharkov Physical Technical Inst. Publ., 2017.
4. Elliot J. P., Flowers B. H. *Proc. Roy. Soc.*, 1957, v. A242, 57.
5. Belyakov A. V. Charge of the electron, and the constants of radiation according to J. Wheeler's geometrodynamic model. *Progress in Physics*, 2010, v. 6, issue 4, 90–94.
6. Belyakov A. V. Macro-analogies and gravitation in the micro-world: further elaboration of J. Wheeler's model of geometrodynamics. *Progress in Physics*, 2012, v. 8, issue 2, 47–57.
7. Belyakov A. V. Nuclear power and the structure of a nucleus according to J. Wheeler's geometrodynamic concept. *Progress in Physics*, 2015, v. 11, issue 1, 89–98.
8. Belyakov A. V. Finding the fine structure of the solutions of complicate logical probabilistic problems. *Progress in Physics*, 2010, v. 6, issue 4, 36–39.
9. https://www.hellma.com/ja/laborbedarf/zertifizierte-referenzmaterialien/messung-der-wellenlaengengenauigkeit/didymium-fluessigfilter
10. Belyakov A. V. The substantive model of the proton according to J. Wheeler's geometrodynamic concept. *Progress in Physics*, 2021, v. 17, issue 1, 15–19.
11. http://nuclphys.sinp.msu.ru/enc/e042.htm
12. Singh P. P., Segel R. E., Meyer-Schützmeister L., Hanna S. S., Allas R. G. *Nucl. Phys.*, 1965, v. 65, 577.
13. Diener E. M., Amann J. F., Paul P. *Phys. Rev.*, 1973, v. C7, 695.
14. Shnoll S. E. Cosmic physical factors in random processes. Svenska fysikarkivet, Stockholm, 2009, 388 pages.